# Effect of Vegetable-Based Polyols in Unimodal Glass-Transition Polyurethane Slabstock Viscoelastic Foams and Some Guidance for the Control of Their Structure–Property Behavior. I

**Benjamin R. Vaughan,[1] Garth L. Wilkes,[1] Dimitrios V. Dounis,[2] Cam McLaughlin[2]**

[1]*Department of Chemical Engineering, Virginia Polytechnic Institute and State University, Blacksburg, Virginia 24061*
[2]*Hickory Springs Manufacturing Company, P.O. Box 2948, Hickory, North Carolina 28603*

Received 31 July 2009; accepted 25 May 2010
DOI 10.1002/app.32865
Published online 9 September 2010 in Wiley Online Library (wileyonlinelibrary.com).

**ABSTRACT:** We investigated the synthesis and structure–property behaviors of two types of vegetable-oil polyols (soy oil and castor oil) and their use in viscoelastic (VE) polyurethane foams (PUFs). This article is the first in a two-part series. In this initial part, we principally address the dynamic mechanical analysis (DMA) behavior of these foams in conjunction with information on the cellular morphology, sol fraction, and rise and reaction temperature profile behavior (the latter two parameters were determined during the foaming process). Particular emphasis is placed on the DMA damping characteristics, which represent one of the most critical parameters in the application of VE PUFs. It is also shown that the damping characteristics could be modified in such foams by the variation of the isocyanate/hydroxyl (×100) index, the addition of plasticizer, and in the case of soy polyols, the soy content. The frequency dependence of the VE PUFs is also briefly addressed. In the second article in this series, which directly follows this article, we further address the details of other relevant physical properties of these same foams in view of their applied nature.  J Appl Polym Sci 119: 2683–2697, 2011

**Key words:** foam extrusion; polyurethanes; structure–property relations

## INTRODUCTION

As the supply of petroleum chemical-based feed stocks decreases and the cost increases, there is continuing pressure to replace these with others that arise from resources that may be less expensive. If such feed stocks can be based on green chemistry and can originate from renewable resources that reduce the energy consumption and carbon footprint of the finished products, this is even more desirable. Furthermore, if these new components can also add any other favorable characteristic properties, this would further enhance their utility if the cost–benefit ratio is suitable. One of the areas of materials science where headway is being made in this regard is that of vegetable-oil-based polyols, which can be used in the commodity products of polyurethane foams (PUFs) or elastomers to replace a portion or possibly all of the common petroleum-based polyether or polyester polyols that comprise the majority of the these products. In the past, there have been many reports on the utility of castor oil as one such vegetable oil for direct use in conjunction with multiple-functionality isocyanates in the synthesis of crosslinked elastomers and higher glass-transition temperature ($T_g$) thermoset materials.[1–5] One advantage of the vegetable oil castor oil, whose generalized chemical structure is shown in Figure 1(A), is that because its triglyceride fatty acid residues are nearly exclusively ricinoleic acid, this allows natural-based hydroxylation, and no further derivatization is necessary beyond suitable purification. As shown in Figure 1(A), all hydroxyl groups are secondary rather than primary and, thus, of lower reactivity than primary hydroxyls. Furthermore, there is a six-carbon inert short olefinic chain that terminates each ricinoleic fatty acid residue; this promotes short dangling ends after any crosslinking reactions that use the hydroxyl functionalities. More will be said about this later in the article. More recently, however, because of the major growth of soybean usage and the much greater portion of the earth where soybeans can be and are being grown, there has been an active focus on the partial incorporation of soy-based polyols into polyurethane (PU) elastomers and all types of PUFs (molded, slabstock, and rigid), and certainly, progress has been made in this

*Correspondence to:* G. L. Wilkes (gwilkes@vt.edu).
Contract grant sponsor: United Soybean Board (to B.R.V. and G.L.W.).

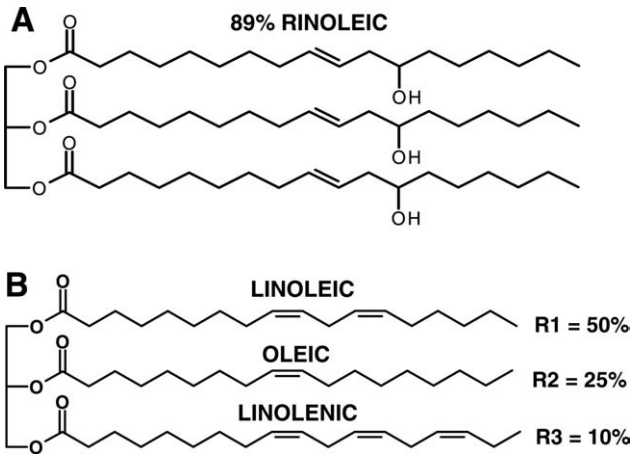


**Figure 1** Generalized chemical structures of (A) castor oil and (B) soy oil. R1 = Linoleic acid, R2 = Oleic acid, R3 = Linolenic acid

regard.[6–11] Of course, because this vegetable oil is not naturally hydroxylated, it must first be derivatized accordingly, and numerous reports and patents have addressed the means and processes of achieving this goal.[12–16] Figure 1(B) depicts an oversimplified schematic of a general triglyceride structure of soy oil; also indicated is that the three major percentages of fatty acid residues are those of linoleic (50%), oleic (25%), and linolenic (10%) acid, all of which possess unsaturation sites that are often used in the promotion of hydroxylation. Because the methodologies of hydroxylation can greatly differ, the nature of the final polyols can also vary in both their chemical characteristics and their molecular weight and distribution.[9] This means the user must be cognizant of such variability when one selects any one of these systems as a possible replacement for another polyol, be it petroleum or vegetable oil.

Certainly, commodity-based PUFs have seen the incorporation of vegetable-oil polyols into their composition for several applications,[9,17,18] and in addition, there have been some reports in the literature on vegetable-oil polyols and their formulation–structure–property behavior.[19–21] However, a unique and widely used PUF that is commonly denoted today in the literature as a viscoelastic (VE) foam is one that has received little attention as a target for vegetable-oil polyol usage. (This same foam has been often referred to as *low-resilience foam, memory foam, dead foam,* and *shape-memory foam.*) It is this subject that we address in this article. More specifically, we attempt to show the effects of the incorporation of soy polyols into VE foams and also the use of castor oil as a polyol to make a VE foam without the use of any petroleum-derived polyols. We also show how the use of a foam index (an index of the excess isocyanate over the required stoichiometric amount to react with all hydroxyl functional moieties) and plasticizer can be used to modify the foam properties and cellular morphology. Finally, we also briefly address effects of the external parameters of humidity, loading rate (frequency), and temperature on the behavior of the prepared foams. Before we address the details of our specific study, it is relevant to provide additional background information from the PUF literature, particularly with an emphasis on VE PUFs.

Flexible PUFs, in general, make up the largest product line for the use of urethane intermediates and, thus, represent a huge commodity product in terms of volume and mass. In fact, the major segment of the PUF market is conventional slabstock foam, which has a global production on the order of 8 million tons a year.[22]

It was Otto Bayer who, in the late 1930s, developed many of the chemical principles for the synthesis of urethane elastomers and foam.[23] Since that time, the consumer has depended particularly on such flexible products for hundreds of everyday applications, and it is often taken for granted that a PUF is a well-understood material. However, a PUF is an extremely complex material from a morphological viewpoint, as is schematically indicated in Figure 2(A).[24] Specifically, slabstock PUF is typically a dual-network material in that there is both a chemically covalent network and a distinct physical microphase-separated network (based on the hard-/soft-segment character of the system); each network strongly influences the structure–property behavior of the final material. One might also say that there is a third network as well, and that is the cellular network comprised of the open-celled nature of the solid portion of the foam with the remaining void space of the cells [see Fig. 2(B)]. This cellular morphology can also greatly influence the physical properties and, through the parameters of strut length and thickness, the cell size distribution/uniformity, residual cell window content (which influences the air flow), and of course, the void content, which is, in turn, coupled to the bulk density. In addition, the microphase structure of the solid portion of flexible slabstock foam arises from the general incompatibility of the lower $T_g$ polyol (generally, its average functionality exceeds the molecular weight of the polyol, typically 2500–6000 Da; this can be used as a means of controlling the soft-phase separation and $T_g$) and that of the higher $T_g$ hard component. The latter component is typically comprised of diisocyanate species, such as toluene diisocyanate (TDI) or methylene diphenyl diisocyanate (MDI), that have been linked together via urea linkages during the reaction of water with the isocyanate functionalities occurring within the foaming process [see Fig. 2(C)].

Typically, flexible conventional non-VE PUFs possess a low $T_g$ in the range of $-50^{\circ}C$, above which

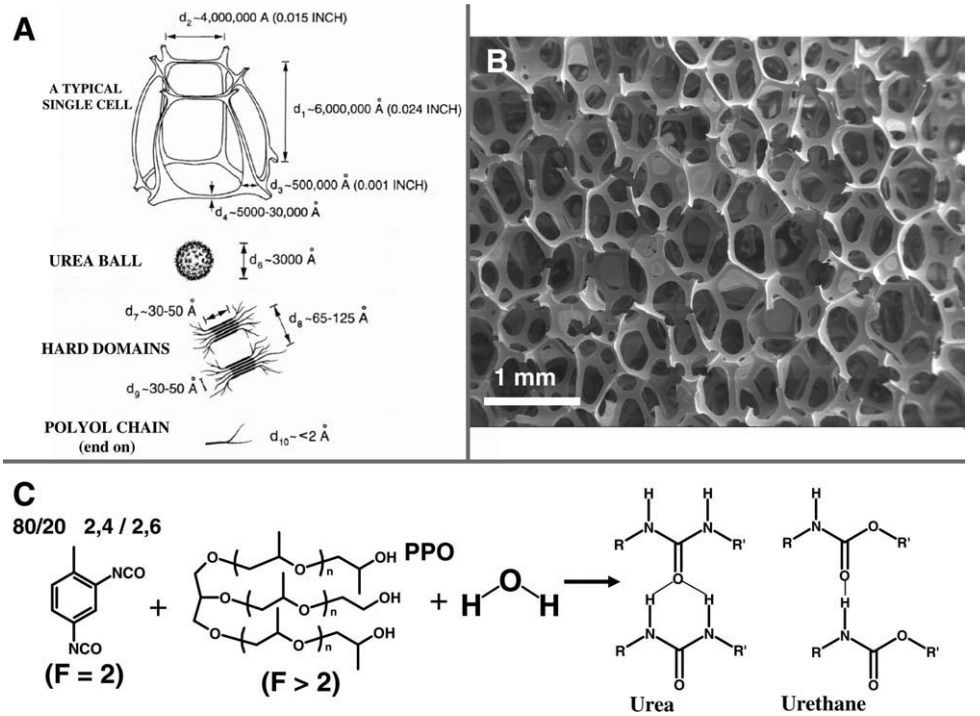


**Figure 2** (A) Morphological features commonly noted on flexible slabstock PUFs at different scale lengths, (B) SEM micrograph of a typical PU slabstock foam, and (C) typical PUF reaction scheme. F = functionality, PPO = poly propylene oxide.

the material displays a rubbery plateau modulus to temperatures in the range of 200°C, at which point reversion of the urethane and urea bonds occurs and/or rapid thermal degradation begins, particularly in an oxygen-containing environment. (Although the so-called hard-segment material has some sign of a $T_g$ in the range of 150°C or higher, because thermal degradation begins in this higher temperature region, one seldom addresses this $T_g$ per se, and that is why, in this article, we also use the phrase *unimodal* $T_g$, which applies to the soft-segment-rich polyol phase.) One of the general physical properties desired by such conventional flexible PUF materials is that they display a high resilience and also respond quickly to deformation when exposed to a changing stress. In other words, a high level of elastic behavior is favored under the use conditions.

In great contrast, for VE PUFs, although they have a related chemistry, a key property of these systems is that they display a much lower resilience and slower response at the use temperature and/or loading rates than are generally associated with typical flexible foams in their cushioning applications. Although full recovery of a VE foam is desired after the load is removed, it is important that the foam is slow in its deformation under load and its recovery after the removal of the load. More specifically, it should display considerable damping; this emphasizes the first portion of the well-known term VE. The temperature and frequency dependence of the damping or mechanical dissipative behavior of polymeric materials is routinely characterized by the use of the standard technique of dynamic mechanical analysis (DMA). Of particular note is that in general, the highest level of mechanical damping (loss/dissipation) of work or energy occurs at the $T_g$ of an amorphous system. Granted, if there are multiamorphous phases, more than a single $T_g$ may exist, and thus, multiple damping peaks can be promoted; these can be used to control the temperature dependence of the mechanical damping. Furthermore, even for a single-phase system, sub-$T_g$ damping transitions may be present, but these are usually of a much lower magnitude because of the lesser degree of localized molecular mobility associated with such transitions.[25,26] Hence, it is apparent that to achieve high damping behavior and low resilience yet still have full recovery following load removal, it is desirable to tune the $T_g$ region of the material such that it is within the application range of temperature and loading rate defined by the use conditions. Quite frankly, these same arguments generally apply to the selection of materials for vibrational or sound damping as well because the goal of each process is to dampen/dissipate the mechanical energy in a material, be it from direct contact dynamic loading or, in the case of sound, by mechanical longitudinal compression waves.[27] Hence, the development of high-damping materials generally requires one to control the magnitude of $T_g$, but more than this, it is

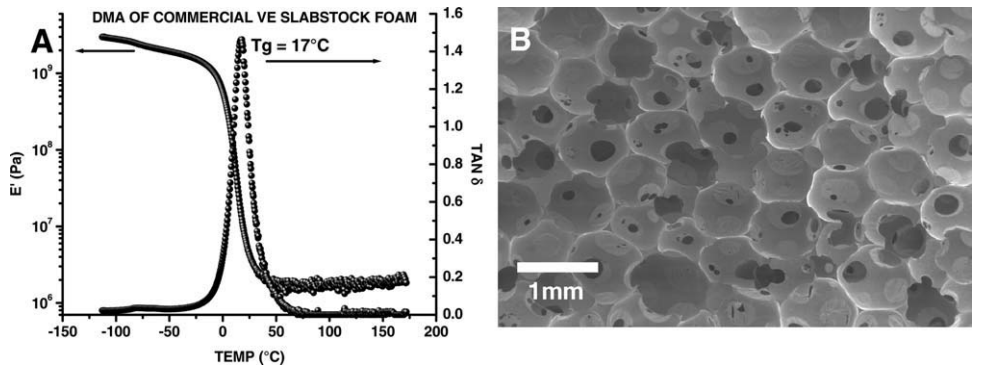


**Figure 3** (A) DMA ($E'$ and tan δ) and (B) SEM micrograph of the top or side of a commercial VE slabstock foam sample.

both the magnitude and the shape of the $T_g$ region (or multiple $T_g$ regions if so desired) that becomes of importance when a VE material, including a VE PUF, is designed.

Sperling and coworkers[27,28] reviewed many of the important molecular principles related to the modification of $T_g$ and its dispersion behavior in polymeric systems. We use some of these principles and others within this article, as will be made apparent. It should be obvious, however, that with respect to the typical flexible non-VE PUF described earlier, which often possesses a single distinct $T_g$ associated with the polyol phase at about −50°C, the movement of that transition to near ambient and the control of its magnitude and shape to facilitate suitable damping behavior for a VE PUF are desirable. Vegetable-oil-based polyols offer some favorable features in this respect, as demonstrated later.

At this point, it is of relevance to provide a few further details to characterize some of the common VE PUFs. Likely, one of the most well-known commercial VE PUFs is that of Tempur-Pedic®, which was stimulated by the pioneering work of Yost and coworkers of NASA in about 1960.[29–31] The DMA of one example of a commercial VE slabstock cushioning product is shown in Figure 3(A). This is but one specific example and may not be representative of all variants of this foam type. However, this VE foam does provide a good example of what we previously discussed regarding the location and nature of the $T_g$ region. Also shown in Figure 3(B) is the scanning electron microscopy (SEM) micrograph of this foam's corresponding cellular texture. As shown in Figure 3(A), the magnitude of the damping parameter, tan δ, whose value is the ratio of the loss modulus ($E$) to that of the storage modulus ($E'$), is in this case, above unity, but the breadth of the transition is quite narrow. Hence, when damping was very high at the $T_g$ peak (17°C at 1 Hz), a relatively small change in the temperature of a few degrees higher or lower not only promoted a pronounced drop in damping but it also had a major effect on the modulus/stiffness of the foam. Specifically, as shown by the data in Figure 3(A), a change from 0 to 10°C promoted a 85% drop in the modulus from $6 \times 10^8$ to $9 \times 10^7$ Pa; this was distinctly significant when we considered that the modulus of a soft rubbery material is about 1 mPa and that of an organic glass is on the order of 1 GPa, that is, a thousand times stiffer. Reflecting back on Figure 3(B), we note that the cellular texture of this example VE foam is quite different relative to the earlier example given in Figure 2(B), which provided an example for a general flexible slabstock PUF; we address such differences in cellular texture later in our two-part report.

Since the introduction of the line of VE products into the market, there have been numerous reports in scientific journals and conference proceedings on some of the features of VE-related foam materials and their fundamental properties; these have all focused on the use of polyols derived largely from petroleum feedstocks.[17,30,32–43] (Glycerin, which could be from natural or synthetic origins, is used in the manufacture of some VE polyols. For simplicity, we refer to these polyols as petroleum-based.) Although most of these have focused on unimodal glass-transition VE foams, Neff et al.[39] addressed dual- or bimodal-$T_g$ VE foams. Bimodal systems are those where the foam displays two polyol $T_g$'s of different damping magnitudes promoted by two incompatible soft-segment phases. The higher tan δ damping magnitude $T_g$ mode was in the range of the use temperature of the material, whereas the lower magnitude $T_g$ was placed at a somewhat lower temperature, the purpose of which then helped maintain some degree of softness and damping below the higher $T_g$ region and also lessened the sensitivity of the modulus when the foam passed through the upper $T_g$ region (see previous discussion). These same researchers also promoted the use of MDI incorporation in conjunction with TDI in the same foam or the production of an all MDI VE product.[38,41] We also addressed the synthesis and structure–property behavior of a number of bimodal $T_g$ VE foams that incorporated soy polyols, and this research will be

**TABLE I**
**Conversion Table for English Units to MKS Units**

| Industry unit | Equivalent SI unit |
|---|---|
| 1 psi | 6894.76 Pa |
| 1 pli | 175.1268 N/m |
| 1 scfm | $4.7195 \times 10^{-4}$ $m^3/s$ |
| 1 pcf | 16.0185 $kg/m^3$ |
| 1 in. | 0.0254 m |
| 1 lb/50 $in.^2$ | 4.4482 N/0.032258 $m^2$ |
| 1 $lb_f$ | 4.4482 N |

reported in another article from our laboratory, which will also expand on the variety of soy-based polyols studied relative to these two articles.[44]

Two us also previously addressed many of the formulation variables that influence the mechanical behavior of largely petroleum-based unimodal-$T_g$ VE foams and their temperature dependence.[34,36] Kageoka et al.,[33] in addition, provided some more detailed studies on the loading rate dependence in conjunction with the temperature variability of VE foams in view of the strong importance of these coupled variables to the actual in-use behavior of such products.

## EXPERIMENTAL

### Unit conversion

A unit conversion chart (Table I) is provided with this report for easy reference. Some of the units used within follow foam industry standard protocol and are, therefore, not reported in MKS = Meter, Kilogram, Second metric units; however, one can use the table provided to convert to MKS units if desired.

### Materials

The petroleum-derived polyol used in this study, Softcel Polyol U-1000, was donated by Bayer MaterialScience (Pittsburgh, PA). The soy-based polyol Agrol 3.0 was donated by Biobased Technologies (BBT, Fayetteville, AR). For simplicity and future reference, we refer to this polyol by its supplier and polyol hydroxyl number (BBT-99).[15] United States Pharmacopoeia grade castor oil (OH# 166, Waltham, MA) was purchased from Fisher Scientific. The catalysts, surfactants, additives, and TDI used in the foam formulation are listed in Table II and were graciously provided by Hickory Springs MFG (Hickory Springs, NC). The catalysts used in the formulation were DABCO T-12 and DABCO 33LV from Air Products (Salt Lake City, UT) and ZF24 from Huntsman Corp. (Allentown, PA). Additives used in this formulation were DP-1022 from Momentive Performance Materials, Salt Lake City, UT Firemaster 550 from Chemtura, and glycerol triacetate (GTA, Middlebury, CT) from Fisher Scientific. The surfactant used in the formulation was L-618 from Momentive Performance Materials. The TDI 80/20 (2,4/2,6 isomer ratio) used for the study was a product of Bayer MaterialScience.

### VE foam synthesis

PUFs were synthesized with the formulation listed in Table II. Approximately 400 g of reagents was mixed with a size #2 ITT CONN blade in a 92-oz polypropylene cup at 2000 rpm and poured into a $10 \times 10 \times 4$ $in.^3$ cake box to rise and cure. The rise height and temperature were monitored and recorded for 5 min with an ultrasonic cone and thermocouple, (Keyence, Osaka, Japan) the latter of which was placed into the reacting system but away from any edge of the box. After 5 min, the foam was placed in an oven at 116°C for 25 min of postcuring in an attempt to better simulate the initial curing conditions in a large commercial bun, that is, with a longer time exposure to the dissipation of the heat of reaction. The samples were conditioned for 3 days at 50 ± 5% relative humidity and 23 ± 3°C before they were cut from the boxes, crushed with mechanical rollers, and conditioned according to ASTM D 3574 for physical testing. The density targeted with the formulation for these laboratory-scale VE foams was 2.7 pounds per cubic foot (pcf), and the density range recorded over all of the samples turned out to be 2.5–3.0 pcf. (In contrast, the density of the commercial VE slabstock sample mentioned earlier, measured with the same methods, and used for some comparison purposes in our two-part report was 5.33 pcf.)

### Characterization methods

Scanning electron micrographs perpendicular to the rise direction were obtained for the foam with a LEO (Zeiss, Oberkochen , Germany) 1550 field emission scanning electron microscope with an SE2 detector set at 10 kV with a WD = working distance of approximately 24 mm.

**TABLE II**
**VE Foam Formulation**

| Reagent | Formula (pph) |
|---|---|
| Polyol | 98.80 |
| DP-1022 | 1.20 |
| Firemaster 550 | 1.00 |
| Water | 1.90 |
| Silicone surfactant (L-618) | 0.50 |
| TD-33 (33LV) | 0.21 |
| ZF24 | 0.21 |
| Tin catalyst (T-12) | 0.03 |
| Tin catalyst (T-9) | 0.00 |
| TDI 80/20 index | 96 |

pph = parts per hundred.

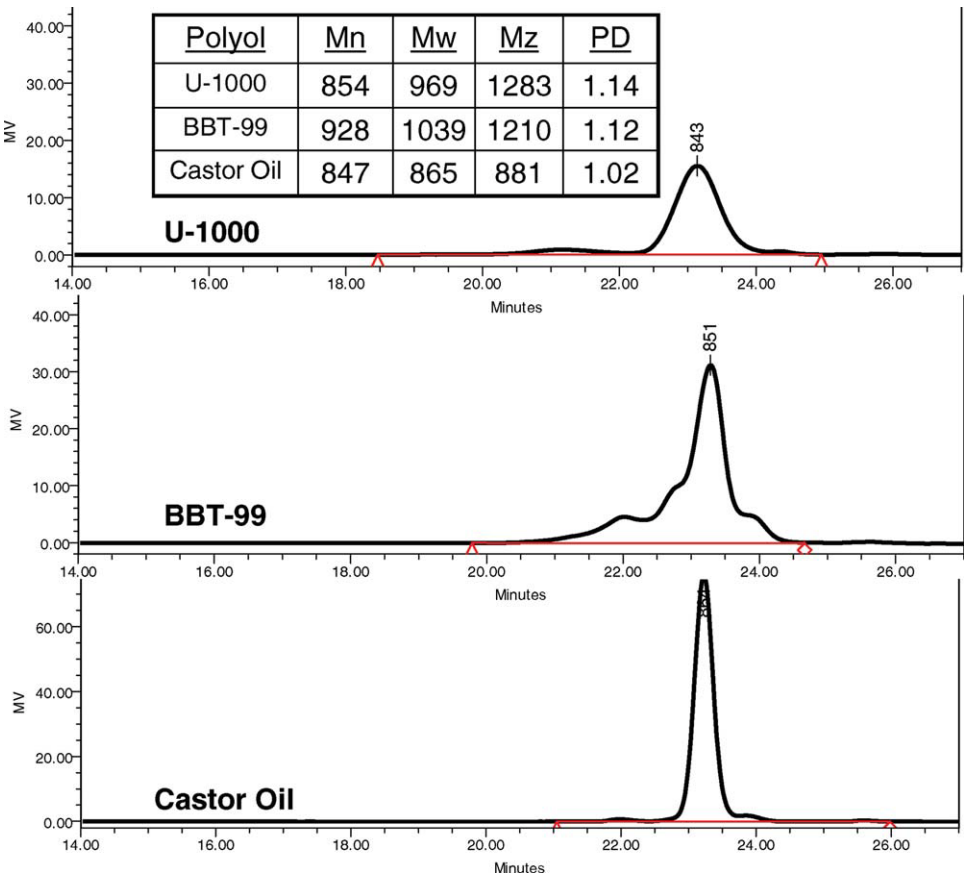


**Figure 4** GPC data for the polyols used in this study. Mn = number average molecular weight, Mw = weight average molecular weight, Mz = z-average molecular weight, PD = polydispersity. [Color figure can be viewed in the online issue, which is available at wileyonlinelibrary.com.]

DMA was performed on rectangular samples approximately $8 \times 8 \times 20$ mm$^3$ on a Seiko SII DMS 210 tensile module equipped with an autocooler for precise temperature control. The samples were tested under a dry nitrogen atmosphere from −110 to 175°C at a heating rate of 2°C/min and a frequency of 1 Hz. Also, selected samples were tested with the same procedure but at frequencies of 0.01, 0.1, 1, and 10 Hz, such that the frequency dependence of $T_g$ could be determined. (Unless otherwise stated, all DMA curves discussed in our article were obtained at 1 Hz.) Because of the difficulty of determining the exact solid cross-sectional area of the cellular solid samples for DMA analysis, the lowest temperature value for $E'$ for all of the foam samples was normalized to $3 \times 10^9$, which was quite representative of the modulus for many noncellular PUFs when they were well below their lowest $T_g$.

We measured the sol fraction by submerging the samples ($34 \times 34 \times 5.5$ mm$^3$) in an excess of dimethylacetamide for 24 h at 50°C with gentle oscillation every 4 h for 5 min to redistribute any concentration gradients. The samples were then removed, blotted, allowed to dry in a convection oven at 60°C overnight, and further dried under full vacuum (30 mmHg) at 65°C for 24 h before the final weight was recorded. The results are reported as the percentage sol fraction.

Gel permeation chromatography (GPC, Milford, MA) was performed on several of the soy polyols used in this study. A Waters Alliance (2) gel permeation chromatograph with two MIXED-D and one MIXED-E PLgel columns was used. The solvent used was chloroform, and the results are based on poly(ethylene glycol) standards. The columns and Waters 2410 refractive index detector were maintained at 40°C during the experiment. The molecular weight information that is reported reflects the relative and not absolute values because comparisons against poly(ethylene glycol) standards were used and also because all polyol molecules, in general, have a branched architecture because of a glycerin-based core. In addition, because the soy-oil and castor-oil polyols were viewed as slightly less polar than the largely petroleum-based propylene oxide polyols, we also realized that this difference may have slightly influenced the relative hydrodynamic volumes of the two types of polyols for the same molecular weights and general molecular architecture.

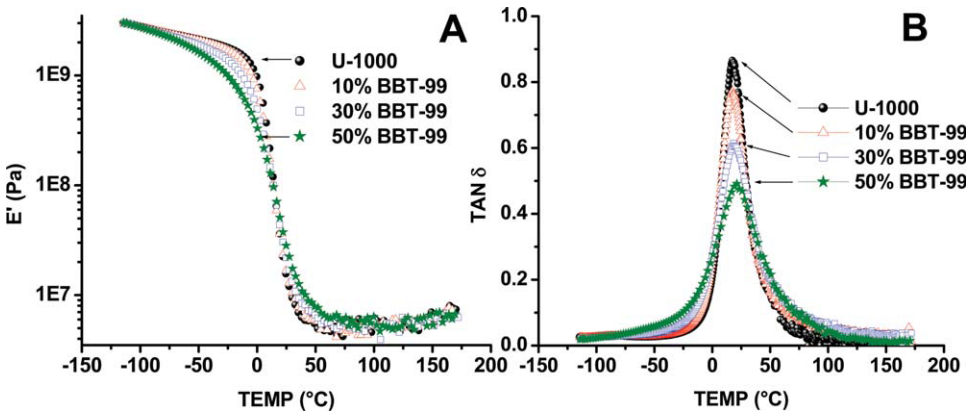


**Figure 5** DMA of (A) $E'$ and (B) tan δ for the U-1000/BBT-99 VE foams. [Color figure can be viewed in the online issue, which is available at wileyonlinelibrary.com.]

Figure 4 shows the GPC traces for U-1000, BBT-99, and castor oil. (The ambient temperature viscosities of the three polyols used in the study were as follows: castor oil = 986 cP, BBT-99 = 440 cP, and U-1000 = 200 cP.) When compared, the three polyols had very similar molecular weights, and all three showed a relatively low polydispersity (1.02–1.14). One subtle difference was observed for the BBT-99 GPC trace, which had some additional shoulders evident around the main peak. These shoulders resulted from a broader range of molecular species present in this material. Recall that this polyol was synthesized via an organic-acid-catalyzed oxidation of soy oil, and this reaction could promote some additional side reactions that could lead to some coupling and the breakdown of the initial soy-oil species.[15,18] Although the polydispersities were somewhat similar for these polyols, castor oil clearly stood out as having the narrowest molecular weight distribution; this may have partially contributed to the difference in the reaction kinetics observed when it was used in foam synthesis. This is addressed in more detail later in the article.

## RESULTS AND DISCUSSION

### VE foams from blends of petroleum polyols with soy polyols

Figure 5(A,B) provides the respective plots of $E'$ and tan δ for the PUFs made only with the petroleum-derived polyol U-1000 and three others that had different contents of BBT-99 soy polyol blended with U-1000. The pure U-1000 material displayed a distinct Tg of 18°C (tan δ peak), whereas there was hardly a change when 10% of the U-1000 was replaced by BBT-99. However, as its content increased to 30 wt %, the Tg moved slightly upward to 22°C. Recall our earlier discussion, however, that only a small change in Tg can, in turn, distinctly affect the damping properties at a specific temperature because a VE PUF is used in its glass-transition region. Furthermore, the addition of the soy polyol had the distinct effect of systematically broadening the Tg tan δ dispersion, which in turn, generally lowers the magnitude of the tan δ peak and, thus, damping at the Tg peak itself. Although one trades off some degree of damping at Tg, the advantage of the slight broadening is that it also lowers the temperature sensitivity of the damping, a point raised earlier in the Introduction. In fact, the integration of the tan δ dispersion for each of the four curves gave essentially identical areas; this suggested that the soy component had the principal effect of only modifying the dispersion shape, which implied that there was likely little change in the microphase morphology of the foam with the change in the composition of the blend of the two polyols. A final point regarding the DMA results is that in view of the single Tg, we suggest that the U-1000 and BBT-99 polyols were miscible because there was no sign of any bimodal behavior in the $T_g$ region.

Figure 6 shows the corresponding SEM micrographs of these four foams as observed down the rise direction. The morphological features of the cellular texture were not greatly influenced by the soy polyol relative to that found for the foam based solely on U-1000. Also, there was a strong similarity in the cellular texture to that given earlier in Figure 3(B), which was shown for the sample commercial VE foam, which in turn, was quite different from the texture of the conventional slabstock PUF [recall Fig. 2(B)]. Indeed, the earlier commercial VE foam and the four U-1000-containing foam textures in Figure 6 imply that the air flow may have been lowered by the lower porosity relative to a more open cellular texture, which could be useful in influencing both the kinetics of compression and the recovery behavior of VE foams under a given load. In other words, this could influence the resilience behavior in that the time dependence of recovery could be affected as could the compression rate for

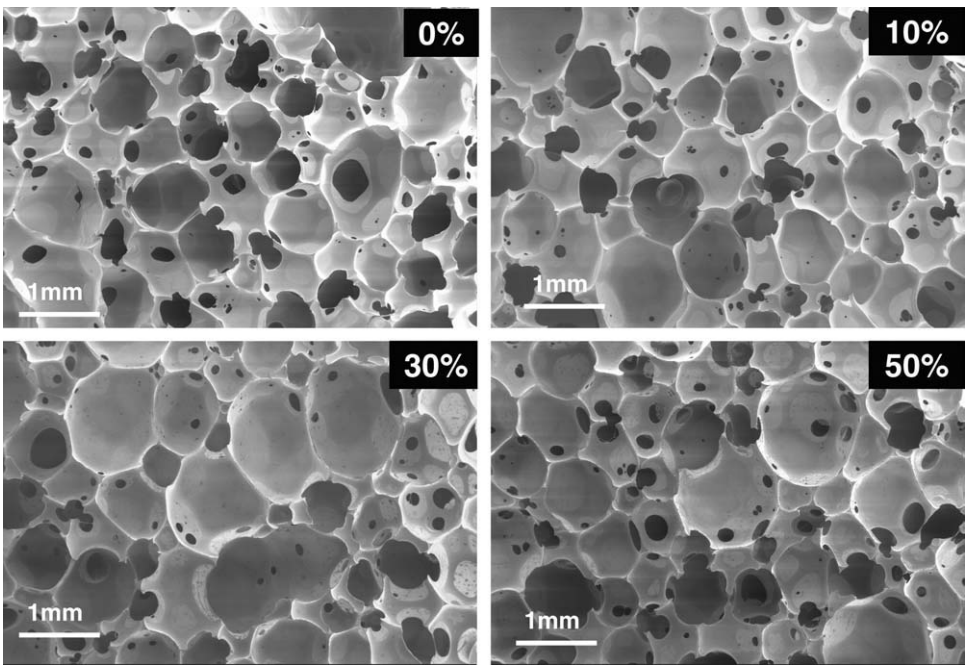


**Figure 6** SEM micrographs of the U-1000/BBT-99 VE foams. The weight weight percent of polyol BBT-99 is given in the upper right-hand corner of each micrograph.

a given load. However, both the compression and recovery behavior were also influenced by several other variables in addition to air flow, such as the crosslink density, $T_g$, and so on, a point we raise again in the second part of this two-part series.

Figure 7 shows the foam height or rise behavior and the temperature within the same four foams during the first 300 s of the reaction. The percentage of soy polyol increased; this did not greatly influence either parameter, although at the highest soy content, the upper or plateau temperature and height were the lowest of the four materials. The cause of this small systematic decrease with increasing soy polyol was not clear but it may have been due to viscosity effects due to the change in the polyol blend composition Furthermore, the viscosity of the BBT-99 soy polyol was higher than that of U-1000, which also tended toward a somewhat lower reactivity rate. This was not a major point because the final four foam densities and general morphological textures were nearly the same in this series.

As shown earlier in Figure 5(B), an increase in the soy polyol content caused a slight increase in $T_g$ and broadened the associated dispersion; it was, therefore, of interest that a decrease in the index of the reaction allowed some offset to this upward shift in $T_g$ and possibly also allowed some control of the dispersion shape. In fact, the use of an index less than unity is common in the preparation of commercial VE foams because it promotes a looser or less crosslinked network, which can generally favorably influence the resilience/damping behavior and other mechanical properties of relevance.[24] Figure 8(A,B) shows the result of a systematic decrease in the index from 102 to 84 for one formulation that contained 30% BBT-99 soy polyol. As one would expect, DMA showed that, indeed, $T_g$ systematically shifted downward with decreasing index and, thus, allowed some control of this important parameter through the index change. Furthermore, the rubbery plateau modulus above $T_g$ also systematically decreased, as should have been the case, because the crosslink density was lower as the index decreased. However,

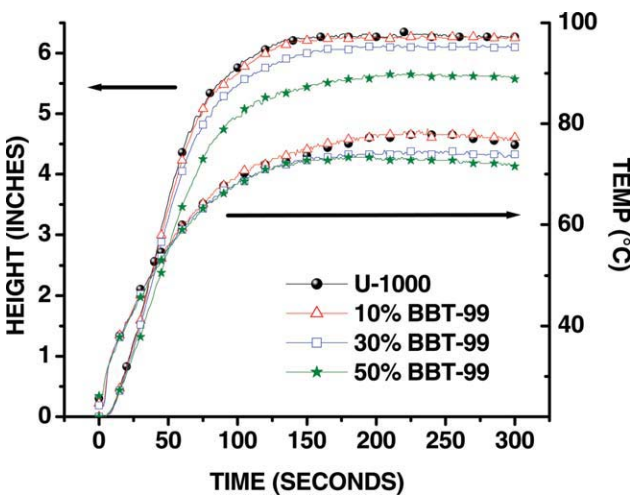


**Figure 7** Foam rise and temperature profiles for the U-1000/BBT-99 VE foams. [Color figure can be viewed in the online issue, which is available at wileyonlinelibrary.com.]

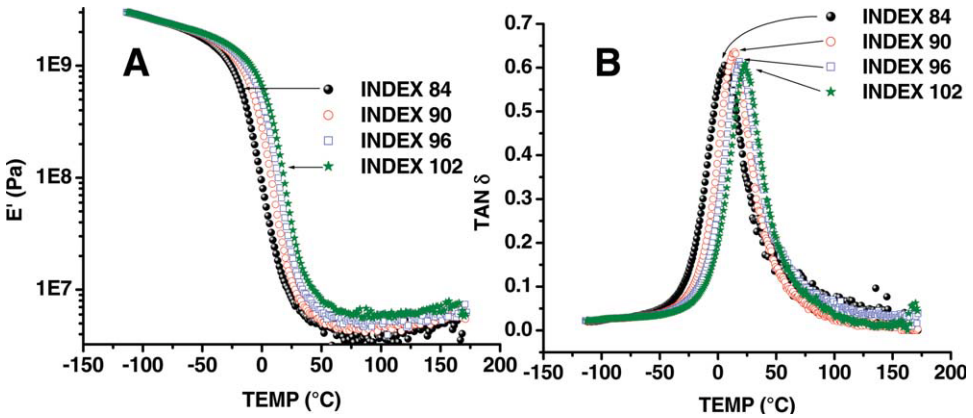


**Figure 8** DMA of (A) $E'$ and (B) tan δ of the 30% BBT-99 VE foams with changing index. [Color figure can be viewed in the online issue, which is available at wileyonlinelibrary.com.]

it was somewhat surprising that the corresponding shape and area of the tan δ dispersion only decreased slightly with a decrease in the index, although the crosslinked network was loosened, and a higher sol fraction was expected. Indeed, this was the case, as shown in Figure 9, where it is noted that upon dimethylacetamide extraction of this series of foams that the sol fraction increased from about 6% to a little over 13% as the index decreased from 102 to 84.

When we focused on the damping behavior, even the magnitude of the tan δ peak was somewhat surprisingly not notably increased, although the drop in modulus from glasslike behavior to that of softer rubbery behavior was greater for a lower index, as was expected on the basis of the decrease in crosslink density. Finally, we show in Figure 10 the SEM micrograph of the lowest and highest index foams. The cellular texture of the low-index system was not significantly altered from that of its highest index counterpart. This was also true for the other two intermediate index foams, and that is why they are not shown, for brevity.

For completeness, we also show in Figure 11 the influence of the index on the foam rise and temperature for the first 300 s of the reaction. A decrease in the index systematically lowered the rate of temperature buildup and the upper or plateau value reached, as was anticipated because there was less reactivity (and, thus, a lower heat of reaction) because of the lower TDI content. Interestingly, the rise, which also decreased slightly, was not greatly affected, and hence, the final bulk densities were nearly the same. This result indirectly supported the common belief that the TDI water reaction is preferred and occurs initially and at a faster rate than the urethane reaction with reduced TDI because the $CO_2$ generation appeared not to be significantly changed in view of all of the foams achieving a nearly comparable density. In summary, it was clear that the index could be used to control the position of $T_g$ and its dispersion within bounds, but of course, other properties were affected, and we address several of these in part II of this two-part series.

We also considered the use of a nonreactive plasticizer as a means of modifying $T_g$ and its dispersion behavior. To do this, we incorporated GTA, which is benign and is used as an excipient in many common products, such as chewing gum. Figure 12(A,B) provides the plots of $E'$ and tan δ for two levels of GTA content and for the nonplasticized system. The plasticization systematically decreased $T_g$, as was anticipated and also lowered the rubbery plateau modulus. Although the location of the dispersion of the tan δ behavior shifted downward as expected, the presence of GTA did little to increase the magnitude of tan δ which was a bit surprising. In contrast and as shown later in this report, the presence of

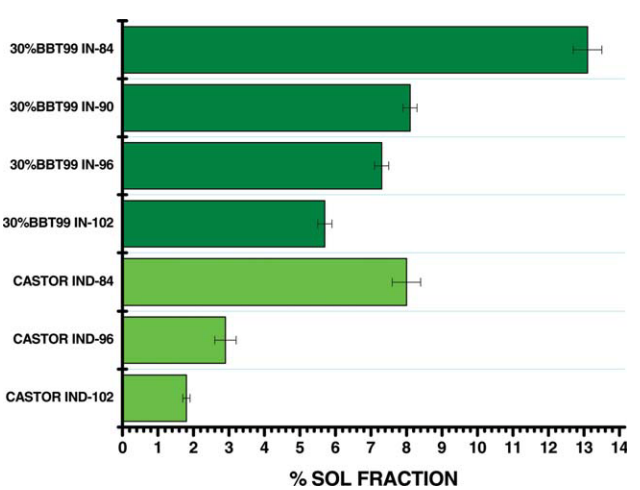


**Figure 9** Sol fraction data for selected VE foam samples in this study. IN and IND = index. [Color figure can be viewed in the online issue, which is available at wileyonlinelibrary.com.]

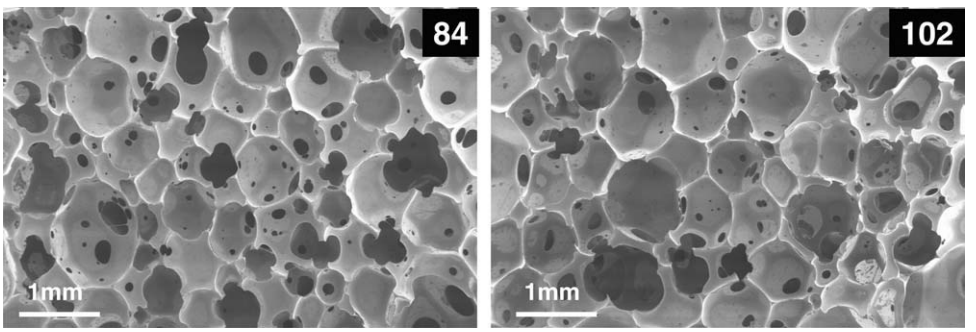


**Figure 10** SEM micrographs of the 30% BBT-99 high- and low-index VE foams. The index values are shown in the upper right corner of each micrograph.

GTA at comparable levels did raise the magnitude of the $T_g$ tan δ peak in the castor-oil-based VE PUFs; this added to the overall damping, which could be viewed favorably for VE applications.

With regard to the rise and temperature behavior of the foams and their dependence on the GTA content, Figure 13 shows that GTA's incorporation systematically lowered the temperature buildup and the upper temperature reached in 300 s. The small decrease in the final reaction temperature was expected because there was a smaller heat of reaction per unit mass of the final formulation because of the incorporation of GTA. The presence of GTA also systematically lowered the height but not to a major extent; this allowed the final foam density to be nearly a constant for all of the members in the series (2.5–3.0 pcf). In fact, because the GTA content had no distinct effect on the alteration of the cellular texture of the soy-containing foam, we did not include the micrographs of this series. However, we show in part II of our two-part report that GTA did have a distinct effect on the recovery kinetics after loading.

To summarize the data presented so far concerning the VE PUFs that incorporated soy polyols, these foams could be made by conventional processing, and their DMA behavior, rise and temperature profiles, and cellular morphology certainly offer the potential for further investigation for applications in the damping materials arena. In the soy-containing foams, no foams above 50% soy content are discussed; when higher contents were made of this particular soy polyol, we found that the $T_g$ peak shifted further upward. This led to a poor VE PUF in the ambient-temperature region. However, certainly, one could easily use a higher molecular weight, lower hydroxyl number soy polyol to lower $T_g$, or it may also be possible to blend a lower $T_g$ compatible petroleum polyol to fine-tune the position of $T_g$. A higher plasticizer content might also be used to lower $T_g$ accordingly. In short, there are a number of possible ways to adjust the position of $T_g$ within these systems. The question remains, however: could one make a VE PUF with no petroleum polyol components at all? To address this question further, we now turn to a discussion of the

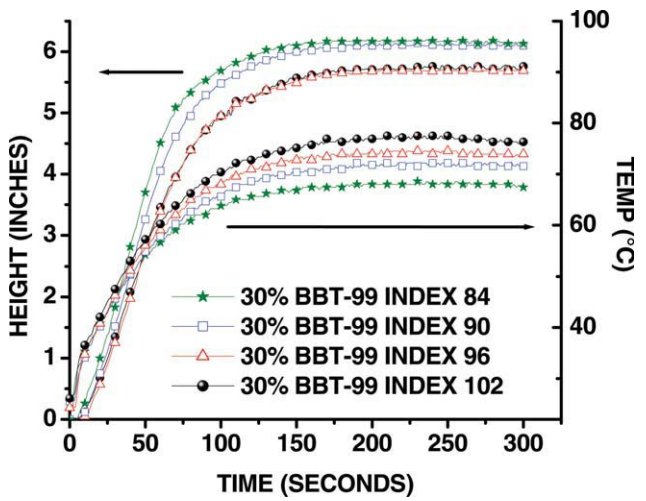


**Figure 11** Foam rise and temperature profiles for the 30% BBT VE foams made with different isocyanate indices. [Color figure can be viewed in the online issue, which is available at wileyonlinelibrary.com.]

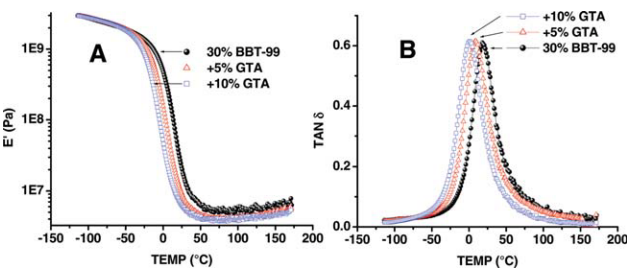


**Figure 12** DMA of (A) $E'$ and (B) tan δ for the 30% BBT-99 VE foams containing GTA. [Color figure can be viewed in the online issue, which is available at wileyonlinelibrary.com.]

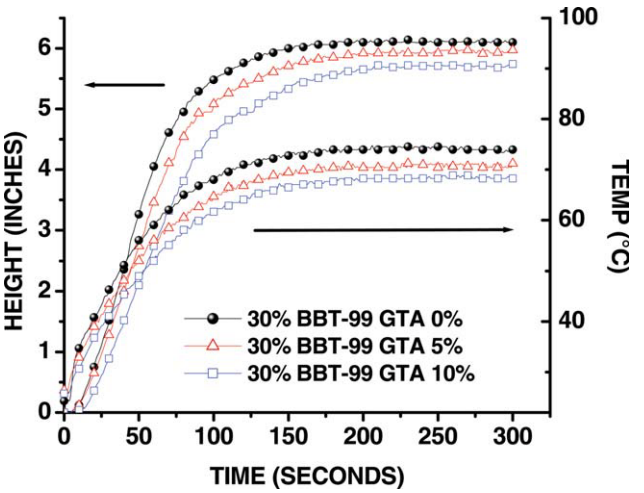


**Figure 13** Foam rise and temperature profiles for the 30% BBT-99 VE foams containing GTA. [Color figure can be viewed in the online issue, which is available at wileyonlinelibrary.com.]

use of castor oil as an alternative vegetable-oil-based polyol that may offer this possibility.

### VE foams from castor oil

Earlier, we mentioned that castor oil is a hydroxylated oil of natural origin; Figure 1(A) shows a simplified schematic of its chemical structure. The basis of why we selected this specific vegetable oil for incorporation into a VE PUF is that our laboratory carried out earlier research on PU elastomers with castor oil, and this polyol provided materials with a $T_g$ distinctly in the range of where that of VE foams are generally located.[45] This prompted us to investigate whether castor oil could also make a fully vegetable-oil-based VE foam with a suitable $T_g$ and how it would compare with VE foams that incorporate soy polyols.

Figure 14(A,B) shows the temperature-dependent behavior of $E'$ and tan δ for the castor-oil foams where the index was varied from 102 down to 84. Interestingly, good cellular foams were produced without difficulty (see Fig. 15, which that provides the corresponding micrographs). We observed that the cellular morphology was quite similar to that already discussed for the sample of commercial VE foam and the foams made from petroleum/soy polyol blends discussed earlier. As shown in Figure 14, indeed, the $T_g$ of these systems did fall in the desired range of VE products [recall Fig. 5(B)] that are used in the ambient region for cushioning. Although the magnitude of the tan δ peak was not as high as those of some of the commercial unimodal $T_g$ VE foams and, in fact, was of somewhat lower magnitude than that for the pure U-1000 polyol foam [again, recall Fig. 5(B)], it was still significant in damping behavior. In addition, it was also similar in shape to the tan δ dispersion for the U-1000 foam determined for the pure U-1000 foam discussed earlier. Furthermore, with decreasing index, the behavior closely followed the same response as did the U-1000 foam, in that the $T_g$ shifted downward. However, in the case of castor oil, the magnitude of tan δ did increase somewhat as the index decreased, and also, the dispersion did broaden somewhat to the lower temperature side. We discuss more in part II of this report on the other physical properties of these foams and how they compared with those discussed earlier.

The corresponding rise and temperature profiles for the castor-oil index series shown in Figure 14 are given in Figure 16, where one notes that although the rise values were in line with those shown earlier for the soy-containing foams, the temperature values were distinctly higher when compared to the profiles obtained for the soy-containing systems. For example, the upper temperature reached above 200°F, whereas the upper most value for the soy system of highest index was only about 170°F. The origin of this higher temperature profile

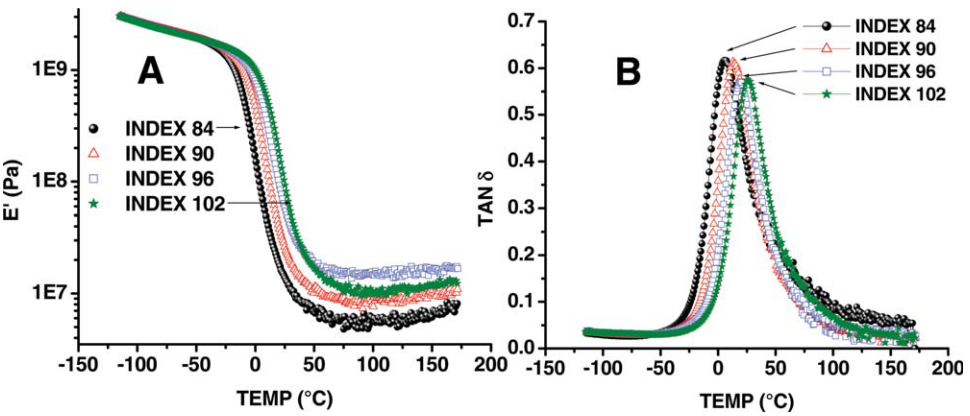


**Figure 14** DMA of (A) $E'$ and (B) tan δ of the 100% castor-oil VE foams with various isocyanate indices. [Color figure can be viewed in the online issue, which is available at wileyonlinelibrary.com.]

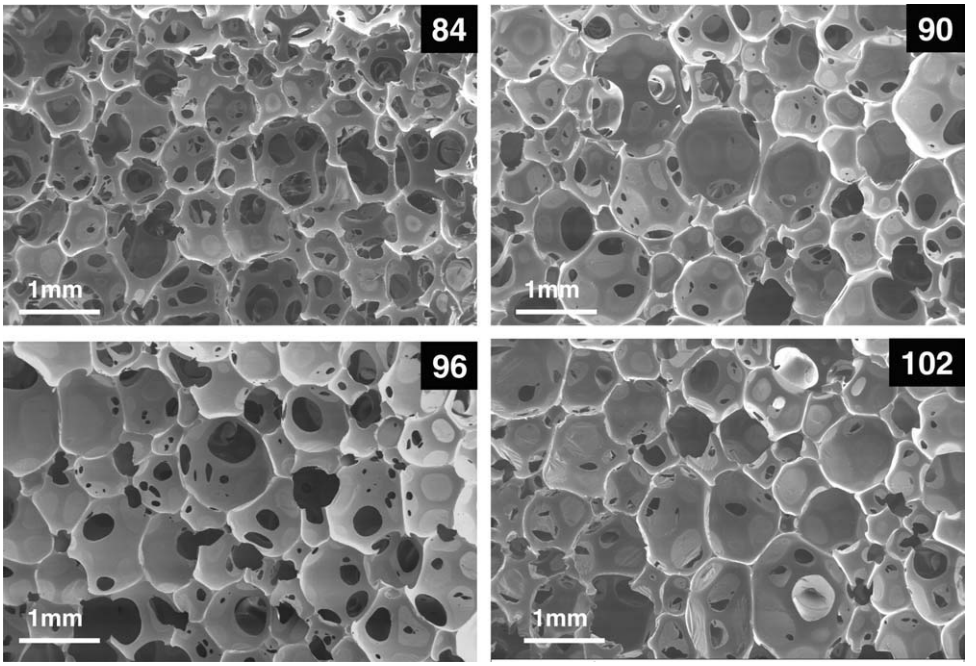


**Figure 15** SEM micrographs of the 100% castor-oil VE foams with various isocyanate indices, as shown in the upper right-hand corner of each micrograph.

relative to the soy-containing systems is not fully understood, but it was clearly reproducible.

The sol fraction content of the castor-oil index series (Fig. 9) showed a distinctly lower content than that which was found for the same index range for the series of VE PUFs containing 30% soy polyol, presented earlier. Specifically, the values for the castor-oil series ranged from about 2 to 8% as the index was varied from 102 to 84, respectively. We strongly believe that the difference in the two systems was due to the fact that each castor-oil-based polyol molecule contained at least one and likely more than two ricinoleic acid residues. Each, of course, contained a reactive hydroxyl group, which allowed for a high probability to react and tie the species into the gel fraction and left fewer dangling nonreactive arms and, thus, less chance for sol species to be present when the index was near 100. This was not the case for the soy-containing material at the same high index; soy-containing polyols typically posses a number of species that are not coupled into the gel fraction because of the lack of reactivity of some of their triglyceride arms, which is caused by an absence of hydroxyl functionalities. Recall the broader molecular weight distribution of the soy polyol relative to the other polyols investigated given earlier in Figure 4. There was also the chance that some of the U-1000 molecular species were also inactive, but we did not probe this issue in any detail.

We also incorporated the GTA plasticizer into the castor-oil systems, and the effect on the DMA characteristics was quite similar to that observed for the earlier soy polyol-containing foams (see Fig. 17). A shift to a lower $T_g$ occurred with increasing plasticizer content, but also, the magnitude of the tan δ peak increased along with a decrease in the rubbery plateau modulus. However, one very different result that arose because of the incorporation of GTA was the effect of this plasticizer on the cellular morphology, as shown in Figure 18, which shows only the two foams incorporating GTA at 8 and 10 wt % (the micrograph for the pure castor-oil foam is shown in

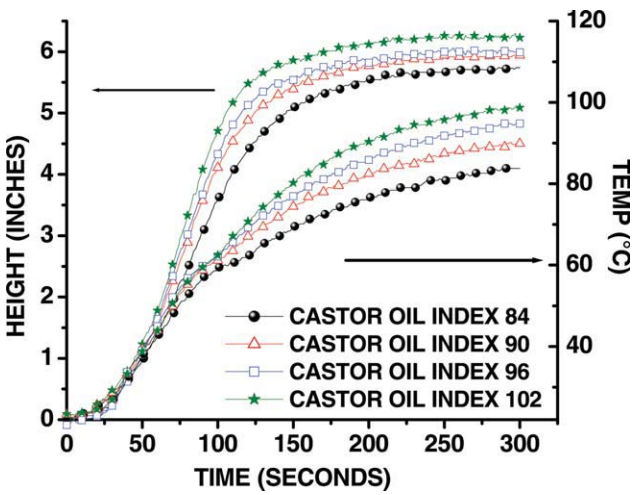


**Figure 16** Foam rise and temperature profiles for the 100% castor-oil VE foams with various isocyanate indices. [Color figure can be viewed in the online issue, which is available at wileyonlinelibrary.com.]

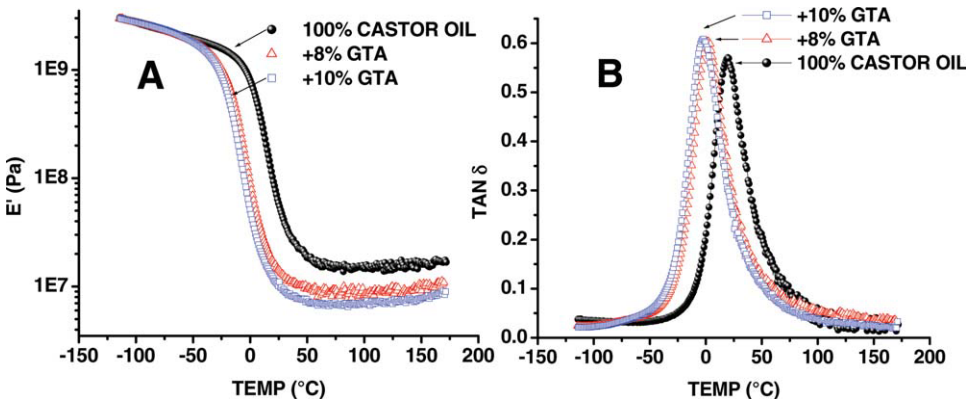


**Figure 17** DMA of (A) $E'$ and (B) tan δ for the 100% castor-oil VE foams containing GTA. [Color figure can be viewed in the online issue, which is available at wileyonlinelibrary.com.]

Fig. 15). We observed that the GTA distinctly opened the cellular structure significantly in the castor-oil foams, although the cell size stayed about the same. Clearly, the plasticizer in the fully castor-oil polyol system displays some characteristics of a cell-opening surfactant in terms of the promotion of cell opening; this was not seen in the soy-containing foams discussed earlier. In part II of our series, we point out how GTA had a distinct effect on the recovery behavior after load removal in compression for both series of foams discussed so far. Finally, we note in Figure 19, which shows the rise and temperature profiles, that although the rise values were little affected, the temperature profiles were again distinctly higher than was observed for the corresponding GTA series in the soy-containing foams; this was consistent with the earlier observations given in Figure 14.

In summary of the castor-oil-based foams, we believe such systems have merit in terms of VE PUF applications, although further work is certainly needed to fine-tune the characteristics of these interesting, fully green, polyol-containing materials. The fact that $T_g$ of the VE foams based on these naturally occurring hydroxylated castor-oil polyols is so near to that of commercial petroleum-based VE foams is particularly striking. This feature, along with the fact that a VE PUF of considerable quality can be easily made without the use of any petroleum polyols, is, therefore, distinctly significant.

### Frequency dependence of Tg for the VE foams

In view of the fact that the properties of VE PUFs are highly influenced by $T_g$ and its dispersion and with the recognition that these specific PUFs, like all flexible PUFs, are VE in nature, it seemed also very relevant to determine the frequency dependence of $T_g$ [as determined by the temperature corresponding to the maximum value of tan δ for each frequency ($T_{max}$)] for these systems. We also wanted to compare the results with a standard commercial VE foam based on petroleum polyols. Hence, DMA of several of our VE foams and the commercial VE slabstock foam we addressed earlier was determined as a function of frequency. Figure 20 shows an example of one of these comparisons, which was typical of all of the VE PUFs that we investigated.

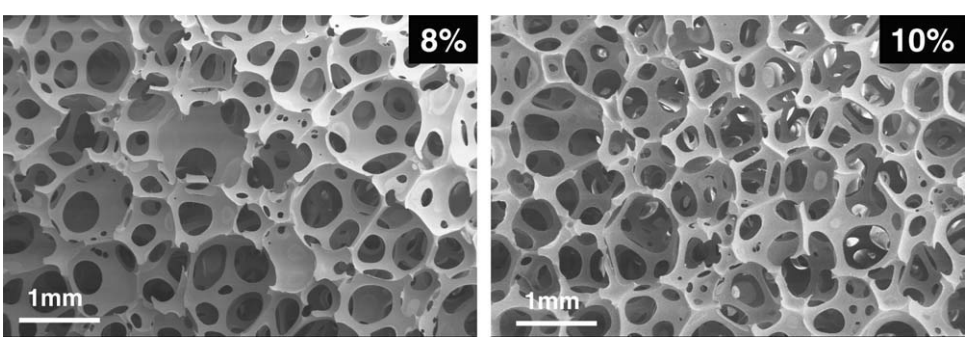


**Figure 18** SEM micrographs of the 100% castor-oil VE foams containing different weight percentages of GTA plasticizer, as shown in the upper right-hand corner of each micrograph.

The figure shows that over the range of frequency studied, the activation energies of the two examples shown were 248 and 257 J/mol, both of which translated to $T_g$ being changed by about 7°C per decade of frequency, which is not uncommon for the behavior of $T_g$. (A very general rule for polymeric materials is that $T_g$ generally changes between 3 and 8°C per decade.) The consequences of being at the higher end of the frequency range is actually viewed as less desirable for VE foams, for this means an increase or decrease in the loading rate of a factor of 10 and will, therefore, shift the $T_g$ dispersion upward or downward, respectively. With this shift, the damping characteristics are distinctly affected, particularly if the $T_g$ dispersion is narrow and of considerable magnitude at its peak. Figure 3(A) shows such a dispersion for the commercial VE foam we used as an earlier example, to which we compared with our VE foams that included vegetable-oil polyols. Such behavior will, therefore, in general, cause the degree of damping to be more dependent on the frequency than a broader dispersion behavior or one with lower magnitude of damping at the $T_g$ peak when other factors are constant. This point is echoed further in part II of this two-part series, which addresses other important mechanical properties, including the standard ASTM damping measurement of ball rebound commonly used for the comparative testing of foams.

## CONCLUSIONS

In summary, we showed that both hydroxylized soybean-oil-based foams and a natural hydroxylized castor oil, a second triglyceride-based vegetable oil, can be used to synthesize VE PUFs with acceptable

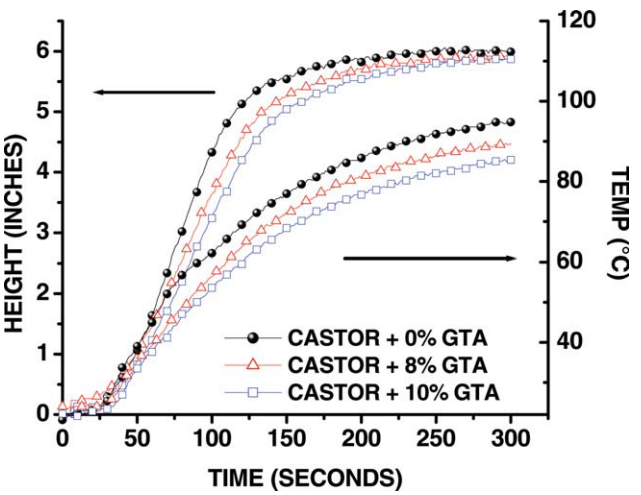


**Figure 19** Foam rise and temperature profiles for the 100% castor-oil VE foams containing various amounts of GTA plasticizer. [Color figure can be viewed in the online issue, which is available at wileyonlinelibrary.com.]

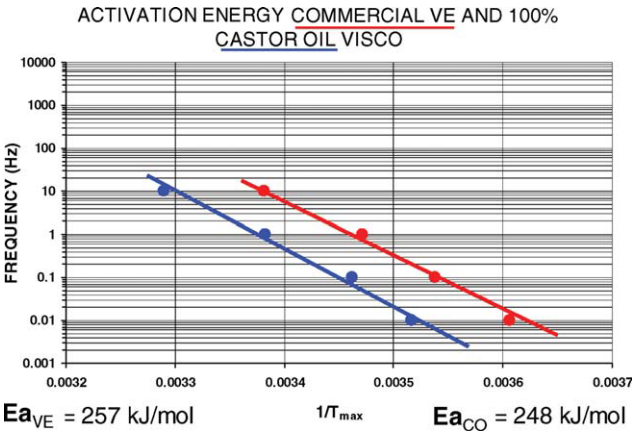


**Figure 20** Plot of the log of frequency dependence of Tg for the castor oil foam (lower curve) and a commercial VE foam (upper curve) sample. [Color figure can be viewed in the online issue, which is available at wileyonlinelibrary.com.]

$T_g$/damping properties, as shown through the principal use of DMA. Although the polyol composition used for the soy-based foam production was a blend of the soy polyol with that of a selected petroleum polyol, the castor-oil-based foams possessed no petroleum polyol. We also showed through SEM investigations that the cell morphology of both the soy-oil- and castor-oil-based VE foams had good uniformity and were of quite similar cell texture as the commercial VE foam. Finally, we also provided some further comparative information on the rise and temperature kinetics of all of these foams. In part II of this report, we address several other important mechanical properties of the same castor-oil- and soy-oil-based foams discussed in this article.

The authors thank Stanley Hager and Richard Skorpenske of Bayer MaterialScience for the donated Bayer polyols and the use of Bayer analytical facilities and for the many helpful discussions and value input associated with this study.

## References

1. Pechar, T. W.; Sohn, S.; Wilkes, G. L.; Ghosh, S.; Frazier, C. E.; Fornof, A.; Long, T. E. J Appl Polym Sci 2006, 101, 1432.
2. Pechar, T. W.; Wilkes, G. L.; Zhou, B.; Luo, N. J Appl Polym Sci 2007, 106, 2350.
3. Tamami, B.; Sohn, S.; Wilkes, G. L. J Appl Polym Sci 2004, 92, 883.
4. Petrovic, Z. S.; Cvetkovi, I.; Hong, D. P.; Wan, X.; Zhang, W.; Abraham, T.; Malsam, J. J Appl Polym Sci 2008, 108, 1184.
5. Sharma, V.; Kundu, P. P. Prog Polym Sci 2008, 33, 1199.
6. Zhang, L.; Jeon, H. K.; Malsom, J.; Herrington, R.; Macosko, C. W. Polymer 2007, 48, 6656.
7. Tu, Y.-C.; Suppes, G. J.; Hsieh, F. H. J Appl Polym Sci 2008, 109, 537.
8. Larre, A.; Barb, D.; Shrock, A.; Bhatacharjee, D. Presented at Polyurethanes 2007 Technical Conference in Partnership with UTECH North America, Orlando, FL, 2008.

9. Herrington, R.; Malsam, J. US Patent Application 2005/0070620.
10. Banik, I.; Sain, M. M. J Appl Polym Sci 2009, 112, 1974.
11. Campanella, A.; Bonnaillie, L. M.; Wool, R. P. J Appl Polym Sci 2009, 112, 2567.
12. Guo, A.; Demydov, D.; Zhang, W.; Petrovic, Z. S. J Polym Environ 2002, 10, 49.
13. Petrovic, Z. S. Polym Rev 2008, 48, 109.
14. Fornof, A. R.; Onah, E.; Ghosh, S.; Frazier, C. E.; Sohn, S.; Wilkes, G. L.; Long, T. E. J Appl Polym Sci 2006, 102, 690.
15. Luo, N.; Newbold, T. (to Biobased Technologies, LLC). US Pat 2008026225.
16. Lozada, Z.; Suppes, G. L.; Hsieh, F.; Lubguban, A.; Tu, Y. C. J Appl Polym Sci 2009, 112, 2127.
17. Babb, D.; Benard, O.; O'Neill, R. E.; Pauperio-Neto, A. (to Dow Global Technologies, Inc.). Braz. Pat. WO/2008/036173.
18. Casper, D. M.; Newbold, T. US Pat 20060041156.
19. Carme Coll Ferrer, M.; Babb, D.; Ryan, A. J. Polymer 2008, 49, 3279.
20. Petrovic, Z. S.; Yang, L.; Zlatani, A.; Zhang, W.; Javni, I. J Appl Polym Sci 2007, 105, 2717.
21. Petrovic, Z. S.; Guo, A.; Zhang, W. J Polym Sci Part A: Polym Chem 2000, 38, 4062.
22. Anderson, A.; Lundmark, S.; Magnusson, A.; Maurer, F. H. J. J Appl Polym Sci 2008, 111, 2290.
23. Uhlig, K. Discovering Polyurethanes; Hanser: Munich, 1999.
24. Herrington, R.; Hock, K. Dow Polyurethanes, Flexible Foams; Dow Chemical: 1997.
25. McCrum, N. G.; Read, B. E.; Williams, G. Anelastic and Dielectric Effects in Polymeric Solids; Dover: New York, 1991.
26. Ward, I. M. Mechanical Properties of Solid Polymers; Wiley-Interscience: London, 1971.
27. Corsaro, R. D.; Sperling, L. H. Sound and Vibration Damping with Polymers; American Chemical Society: Washington, DC, 1990.
28. Sperling, L. H.; Fay, J. J. Polym Adv Technol 1991, 2, 49.
29. Yost, C. A.; Oates, R. W. NASA Contractor Rep 1969, Nov, 1.
30. PFA IN•TOUCH 2003, 11, 1.
31. Turner, J. Forty-Year-Old Foam Springs Back With New Benefits. NASA Spinoff [Online] 2005. http://www.sti.nasa.gov/tto/Spinoff2005/ch_6.html.
32. Lutter, H. D.; Mertes, J.; Zschiesche, R. Presented at the Polyurethanes World Congress, Nice, Sept 1991.
33. Kageoka, M.; Inaoka, K.; Kumaki, T.; Tairaka, Y. J Cell Plast 2000, 36, 15.
34. Hager, S.; Skorpenske, R. Proceedings of the Polyurethane Foam Association Technical Program, Arlington, VA, May 2001; 2001.
35. Tobushi, H.; Okumura, K.; Endo, M.; Hayashi, S., J Intel Syst Str 2001, 12, 283.
36. Hager, S.; Skorpenske, R.; Triouleyre, S.; Joulak, F. J Cell Plast 2001, 37, 377.
37. Farkas, P.; Stanciu, R.; Mendoza, L. J Cell Plast 2002, 38, 341.
38. Neff, R.; Green, T.; Apichatachutapan, W.; Smiecinski, T. In 2003 Polyurethanes Expo Proceedings, Orlando, FL; p 311.
39. Neff, R.; Dakin, S.; Green, T.; Gummaraju, R.; Smiecinski, T. Presented at Polyurethanes Conference, Las Vegas, NV, Oct 2004.
40. Delk, V.; Polk, R.; Prange, R.; Aguirre, F. Proceedings of the Annual SPI Polyurethanes Technical/Marketing Conference, Las Vegas, NV, 2004; 2004; p 35.
41. Smiecinski, T. M.; Neff, R. A. Proceedings of the API Polyurethanes Technical Conference, Salt Lake City, UT, 2006; 2006; p 405.
42. Butler, D.; Obi, B.; Elwell, M.; Sonney, J. M.; Wuilay, H.; Cosman, J. Presented at CPI 2007, Orlando, FL, 2007.
43. Kintrup, S.; Treboux, J. P.; Mispreuve, H. Presented at API Polyurethanes 2000 Conference, Boston, MA, Oct 2000.
44. Vaughan, B. R.; Wilkes, G. L.; Dounis, D. V.; McLaughlin, C. J Appl Polym Sci 2010.
45. Pechar, T. W.; Das, S.; Depolo, W.; Wilkes, G. L. Presented at Thermosets Plastics TAP Meeting, Detroit, MI, 2007.